Advanced Sustainable Systems

ADVANCED SUSTAINABLE SYSTEMS
www.advsustainsys.com

RESEARCH ARTICLE

Hydrophobic Ionic Liquid-Doped Poly(3-hydroxybutirate) Membranes as Sustainable Systems for Efficient Dye Pollutant Removal and Photodegradation

Salvatore Marullo[1] | Luigi Cino[1] | Chiara Laferrera[2] | Vincenzo M. Marzullo[2] | Giuliana Impellizzeri[2] | Francesca D'Anna[1]

[1]Dipartimento STEBICEF, Sezione di Chimica, Università degli Studi di Palermo, Palermo, Italy | [2]CNR-IMM, Via Santa Sofia 64, Catania, Italy

Correspondence: Salvatore Marullo (salvatore.marullo@unipa.it) | Francesca D'Anna (francesca.danna@unipa.it)

Received: 2 February 2026 | **Revised:** 17 July 2026 | **Accepted:** 22 July 2026

Keywords: ionic liquids | polymer membranes | poly(3-hydroxybutirate) | photocatalysis | water treatment

ABSTRACT

Contamination of water bodies is one of the pressing issues of modern society. In this context, to achieve sustainable removal of pollutants from wastewater, the authors prepared hybrid membranes based on biomass-derived poly(3-hydroxybutirate) doped with hydrophobic imidazolium-based ionic liquids differing for the alkyl chain length. Membranes were easily prepared, without synthetic steps, and were characterized by surface roughness, hydrophobicity/hydrophilicity and morphology. Then, these materials were investigated for their ability to remove cationic, neutral and anionic dye pollutants from water. The materials showed fast and thorough removal of most dyes, particularly cationic and neutral ones. Adsorption process was investigated in terms of mechanism and kinetics determining the adsorption isotherms and rate. The best results were obtained for methyl violet with maximum adsorption capacity of 132 mg/g, and the performance of the systems proved comparable to the one of related systems reported in the literature. The best-performing membrane was reused nine times without significant loss in removal efficiency or intermediate washing. To minimize the waste generated by the adsorption process, the membranes were further doped with a photocatalyst like TiO_2 and employed to degrade dyes in water solution, finding that they are effective and recyclable catalysts, especially toward cationic dyes.

1 | Introduction

Water pollution resulting from human activities is a constant source of concern in present-day society, given that water is an essential and limited resource. Consequently, preservation of existing water sources and remediation of polluted water bodies are mandatory to ensure acceptable standards of living. This has driven research to develop efficient strategies and methodologies to remove pollutants from contaminated water bodies. Among the different methodologies that can be used to tackle this issue, such as advanced oxidation [1], membrane filtration [2], or biological treatments [3], adsorption-based methodologies [4] have risen to a certain prominence, due to beneficial characteristics, like low cost and energy demand, simplicity of process, removal efficiency, and selectivity, often coupled with recyclability. Another advantage of adsorption methods is the possibility to employ a wide range of different materials, depending on the nature of the pollutant to be removed.

Among the various sorbents that can be successfully used, polymer membranes have recently emerged as sustainable materials for water treatment [5]. This arises from the peculiar advantages of polymer membranes over other kinds of sorbents, such as high adsorption capacity and selectivity toward some pollutants

[6, 7], coupled with easy separation and scalability to treat larger volumes of liquid phase [8]. Compared with other sorbents, membranes present the peculiar possibility of dual use, both as adsorption material or ultrafiltration [9]. Recent developments in the field include the use of nanowoven polyethylene terephthalate fibers to obtain adsorptive membrane for the removal of dyes from water or polymer [10] membranes for the fractionation of dyes and inorganic salts [11]. In both cases, the porosity of the membranes exerts a critical role [10]. Finally, to address the issue of sustainability, the judicious choice of the polymer and component used, coupled with their recyclability, makes easy to design membranes that are composed by environmentally benign components [12, 13].

Furthermore, polymer membrane-based adsorbents can be further modified in a straightforward way by doping them with relatively small amounts of different components, giving rise to hybrid polymer membranes. Such treatments often improve the characteristic of the parent membrane, in terms of mechanical resistance, adsorption or filtration efficiency, resistance to fouling as well as overall long-term stability [14]. Examples of such modifiers include biopolymers like chitosan or cellulose, transition metal oxides or nanomaterials like carbon nanotubes or graphene [15].

Another kind of dopant that can be used is constituted by ionic liquids (ILs). These are low melting organic salts, conventionally lower than 100 °C, which in many cases are liquid at room temperature, providing a class of nonconventional solvents entirely constituted by ions and possessing beneficial characteristics from a sustainability point of view, like negligible volatility and flammability [16, 17].

Consequently, ILs endowed with suitable ions can be successfully used as dopants for polymer membranes to enhance their properties. In this context, protic imidazolium-based ILs were used as dopants for polyimide membranes enhancing their proton conductivity and water sorption ability [18]. In another example, hydrophobic ILs embedded in poly(vinyl chloride) membranes improved the removal ability and selectivity for metal ions in wastewaters [19].

Based on these considerations, we prepared two hydrophobic IL-doped poly(3-hydroxybutirate) (PHB) membranes by solvent casting. In particular, we considered hydrophobic imidazolium-based docusate ILs $[C_1C_8Im][Docusate]$ and $[C_1C_{10}Im][Docusate]$, reported in Figure 1a. These ILs were chosen for their relatively long alkyl chains, to enhance hydrophobicity, with the docusate anion used not only for its hydrophobicity but also on the grounds of its low toxicity, which enables its use in pharmaceutical formulations [20].

We chose to use PHB (Figure 1b) as it is a natural biodegradable polymer that can be produced from lignocellulosic feedstocks, which is beneficial from the standpoint of sustainable chemistry [21, 22] and fulfills the sixth principle of Green Chemistry. This polymer is generally claimed as a sustainable alternative for non-biodegradable plastics, like polypropylene, and finds application in different areas, like pharmacology, biomedical, packaging, and agricultural industries [23–25]. Consequently, its reuse in a second life, like the production of membranes for environmental remediation, can represent a way to address concerns due to its production cost and extraction [26].

We characterized the morphology of the membranes by scanning electron microscopy (SEM), and the surface roughness was investigated by optical profilometry. In addition, hydrophobicity/hydrophilicity of the surface was investigated by contact angle measurements. Then, we employed both membranes as sorbents for the removal of dyes from aqueous solutions. In particular, we considered anionic, cationic and neutral dyes, namely, rhodamine B (RhB), methylene blue (MB), eosin yellow (EY), bromocresol green (BG), methyl orange (MO), methyl violet (MV), and bromothymol blue (BB), reported in Figure 1c.

After optimizing parameters, such as the amount of IL dopant and the surface of membrane exposed to the aqueous phase, we studied the adsorption process in terms of adsorption kinetics, by time-dependent adsorption tests and obtained mechanistic information, by determining the adsorption isotherms as well as the maximum adsorption capacities. We also evaluated the recycling of the materials, finding that the best membrane was reusable nine times without loss in efficiency or need of intermediate washing.

Considering that the adsorption process generates a polluted material, we also evaluated the possibility of degrading the dyes, using a low-impacting methodology like photocatalysis [27, 28]. To this aim, the best-performing membrane, PHB/$[C_1C_{10}Im][Docusate]$, was further doped with a photocatalyst like TiO_2 and employed as catalyst for the photodegradation of cationic dyes in aqueous solution, such as RhB and MB. TiO_2 nanoparticles have been recently used for the degradation of emerging pollutants [29, 30], and the system proposed herein could represent a viable strategy to further address this issue. Interestingly, $[C_1C_{10}Im][Docusate]$/PHB/TiO_2 hybrid membrane enables almost thorough and fast degradation of the dye, with a good degree of recyclability.

2 | Results and Discussion

2.1 | Membrane Preparation and IL Content Optimization

The IL-doped polymer membranes were prepared by solvent casting, dissolving 500 mg of PHB and the suitable amount of IL (see later), in 12 mL of chloroform, heating at 50°C for 30 min, until obtaining a clear solution, which was subsequently poured in a Petri dish and left to cool at room temperature overnight. Different volumes of chloroform were tested, and 12 mL was the minimum one allowing dissolution of the mixture. The membranes obtained were uniform opaque solids. A schematic depiction of the preparation of the membranes and a representative picture of a membrane are reported in Figure 2.

Subsequently, we ran preliminary adsorption tests aimed at optimizing the amount of IL in the membranes. Initially, we assessed the resistance of the membranes, with 60 wt.% of IL, when put in contact with water, looking for the possible leaching of ILs in the aqueous phase. To such aim, we put 30 mg of each material in contact with 1 mL of D_2O for 24 h, at 25°C.

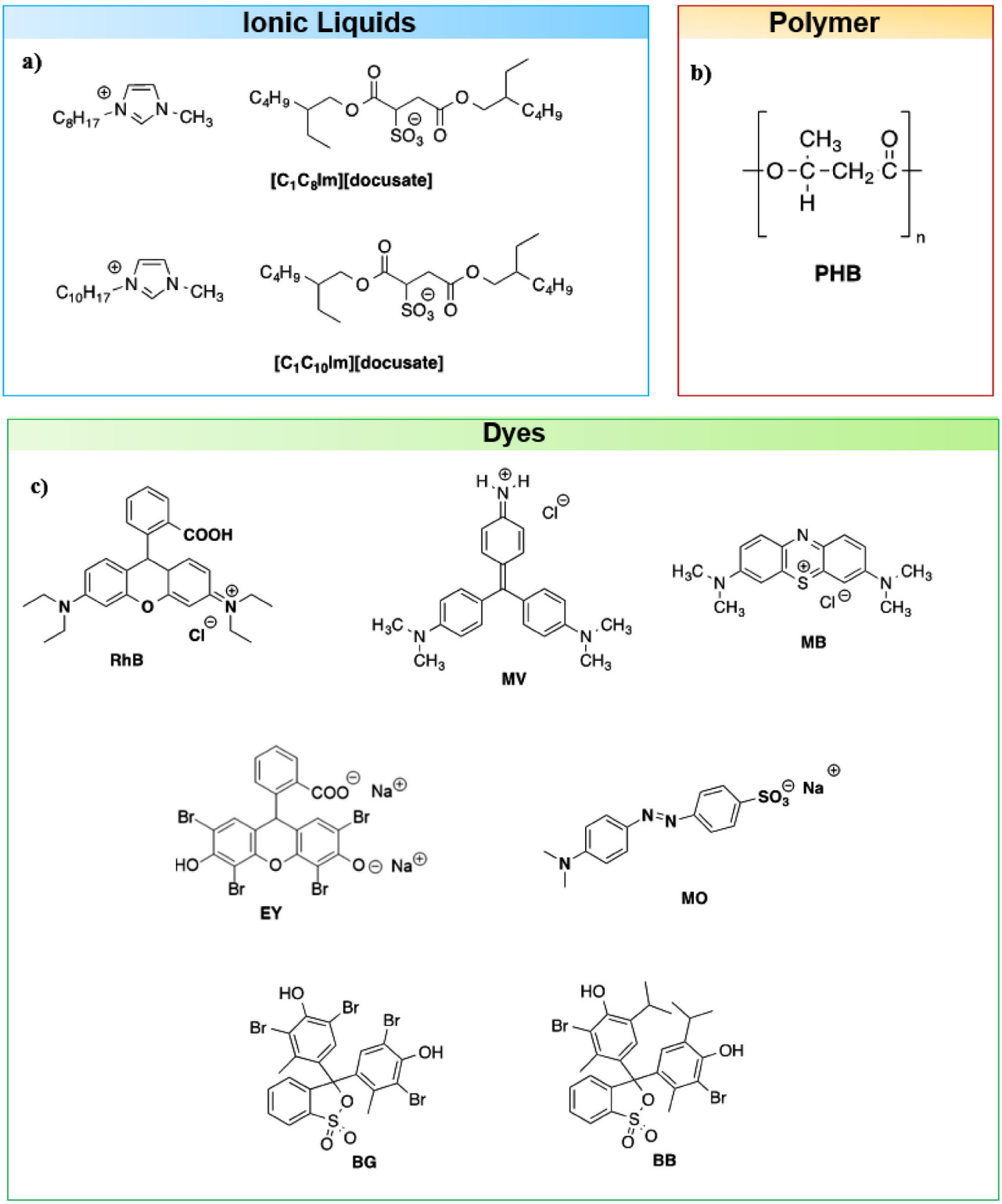

FIGURE 1 | Structures of (a) hydrophobic ionic liquids, (b) polymer, and (c) dyes.

Subsequently, we recorded the ^{1}H-NMR spectra of the aqueous phases, reported in Figure S2. In both cases, no significant amount of IL was leached in the aqueous phase, prompting us to conduct static dye adsorption tests.

Subsequently, we ran a preliminary adsorption test to compare the sorption ability of the hybrid membranes with the pristine PHB film, devoid of IL. In particular, we put into contact, at 25 °C, 300 mg of each solid with a 1.0×10^{-4} M solution of RhB for 4 h, after which we measured the removal efficiency, RE%. The results obtained, showed that RE% was 12% in the presence of the PHB pristine film, while it increased to 50% and 52% when the hybrid membranes doped with $[C_1C_8Im][Docusate]$ and $[C_1C_{10}Im][Docusate]$ were used, respectively. These findings

FIGURE 2 | Schematic depiction of (a) membrane preparation and (b) representative picture of an IL-doped PHB membrane.

clearly show that the presence of ILs is beneficial for the removal of dyes, and ILs actively assist the adsorption process, due to their affinity with this kind of pollutants [31–33]. To evaluate the effect of the amount of IL doping on the membrane, and to obtain a first indication of their removal ability, we prepared membranes using 500 mg of PHB and variable amount of both ILs, ranging from 30 to 80 wt.%, with respect to the polymer. The membranes, (rectangular sections 2 cm × 1 cm) were then put in contact with 10 mL of dye aqueous solutions (1.0×10^{-4} M) for 4 h at 25 °C. The plots of removal efficiency in the presence of each dye are reported in Figure S3, while their values are summarized on Table S1.

Examination of the results reported in Figure S3 shows clearly that both membranes have much higher affinity for the cationic (RhB, MV and MB) and neutral (BB and BG) dyes compared to the anionic ones (EY and MO). We also encountered this higher affinity for cationic over anionic dyes in other IL-based sorbent materials [32, 34]. In addition, for both membranes, and for all the dyes considered, increasing the amount of IL improves the adsorption ability up to 60 wt.%, after which the RE% plateaus. Therefore, for the rest of the study, and the following characterization, membranes were prepared with this amount of ILs. A closer inspection of the plots reported in Figure S3 reveals that, going from the $[C_1C_8Im]$[Docusate]/PHB to $[C_1C_{10}Im]$[Docusate]/PHB, slightly improves the removal efficiency for the anionic dyes, which approaches 30% compared with the negligible adsorption in the presence of the former membrane. Hence, not only the presence of ILs is beneficial for the adsorption of dyes, but a rather subtle structural variation, as a longer alkyl side chain on the imidazolium cation, is able to significantly modulate the performance of the ensuing material.

2.2 | Membrane Characterization

Initially, we set out to characterize the materials obtained, probing their surface by SEM, obtaining the images reported in Figure 3.

The SEM images reported in Figure 3 show that in both cases the materials obtained exhibit a uniform surface characterized by a significant roughness. To better analyze these features, we carried out a surface scanning with a profilometer, able to probe the heterogeneity and roughness of the surface. The images of the surface scan are reported in Figure 4, while the values of the parameters extracted are reported in Table 1.

Examining the magnitude of the profile parameters reported in Table 1 shows a marked difference in roughness as a function of the IL present in the membrane, with $[C_1C_{10}Im]$[Docusate] inducing a significantly higher surface roughness, as exemplified by the values of the average roughness, R_a increasing for more than one order on magnitude on going from $[C_8C_{10}Im]$[Docusate] to $[C_1C_{10}Im]$[Docusate]. The values of the other parameters are consistent with this observation. This shows the potential of ILs to modulate the surface properties of the material obtained, by a subtle structural variation, such as the lengthening of the alkyl side chain in the imidazolium cation.

To further probe the features of the membrane surface, in terms of hydrophilicity/hydrophobicity, we carried out static water contact angle measurements. Images pertaining to the contact angle measurements are reported in Figure 5.

Also in this case, a significant effect of the ILs on the properties of the membrane surface can be detected, consisting in an increased surface hydrophobicity on going from the membrane doped with $[C_1C_8Im]$[Docusate] to the one doped with $[C_1C_{10}Im]$[Docusate], since the water contact angle are equal to (72 ± 3)° and (86.7 ± 0.2)° for $[C_8C_1Im]$[Docusate]/PHB and $[C_1C_{10}Im]$[Docusate]/PHB, respectively. Therefore, this further supports the observation that ILs can effectively modulate the surface features of the materials, and the trend observed is in line with the higher hydrophobicity of the $[C_1C_{10}Im]$[Docusate] ILs, because of its longer alkyl chain. In this latter case, the $[C_1C_{10}Im]$[Docusate]/PHB membrane can be considered having an actual hydrophobic surface, given the closeness of the water contact angle to 90° [35].

2.3 | Dye Adsorption Tests: Optimization of Experimental Conditions

After characterizing the IL-doped PHB membranes, we set out to systematically investigate their ability to act as sorbents for the removal of dye pollutants from aqueous solutions.

As a further experimental parameter, we investigated the effect of the surface area of the membrane exposed to the dye solution. More specifically, we employed rectangular sections of each membrane, immersed for a height of 2 cm in the solution, at different widths, ranging from 1 to 1.6 cm. The results obtained after 4 h are reported in Figure S4 and Table S2.

As can be seen from the plots reported in Figure S4, increasing the membrane width does not induce any improvement in the removal efficiency of each dye. For this reason, in the following experiments we used only rectangular sections with a width equal to 1 cm.

Finally, we wanted to preliminary assess the performance of our membranes as a function of the initial concentration of dye

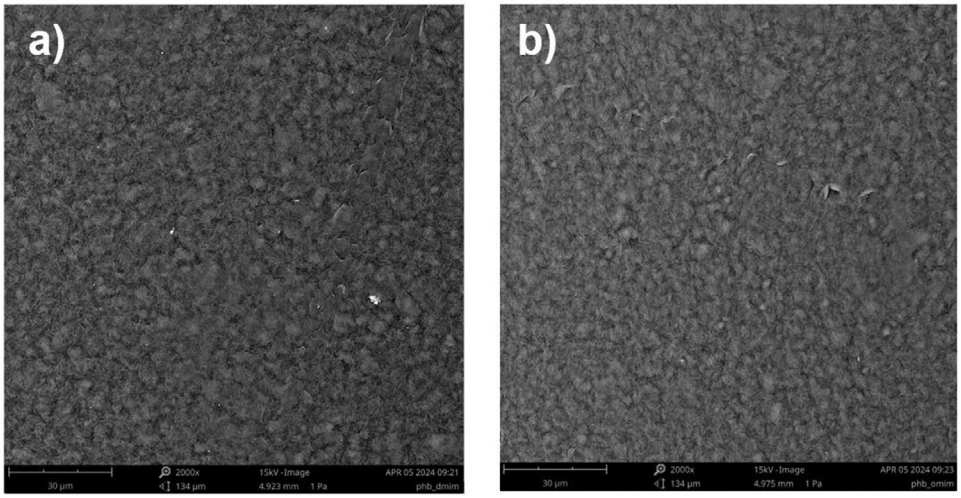

FIGURE 3 | SEM images at 2000× magnification of (a) $[C_1C_{10}Im][Docusate]$/PHB and (b) $[C_1C_8Im][Docusate]$/PHB membrane, containing 60 wt.% of IL.

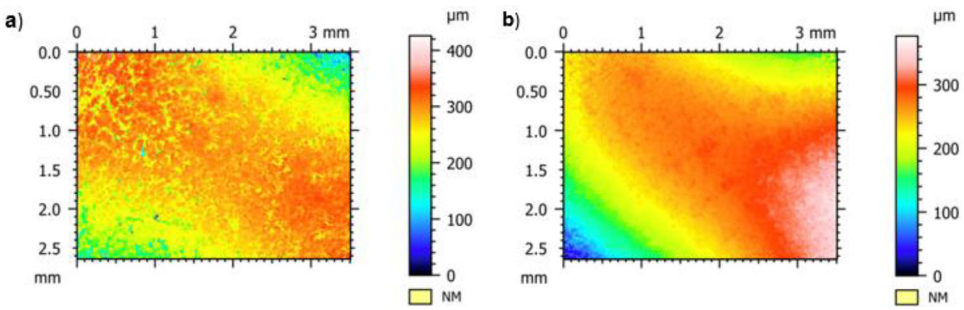

FIGURE 4 | Surface profiles of (a) $[C_1C_{10}Im][Docusate]$/PHB and (b) $[C_1C_8Im][Docusate]$/PHB membrane., containing 60 wt.% of IL.

TABLE 1 | Amplitude parameters in roughness profile for the two IL-doped PHB membranes, containing 60 wt.% of IL.

Amplitude Parameter	$[C_1C_8Im][Docusate]$/PHB	$[C_1C_{10}Im][Docusate]$/PHB
R_a Average roughness (µm)	1.72	30.87
R_q Root mean square roughness (µm)	2.09	34.23
R_v Maximum valley depth (µm)	3.97	63.42
R_p Maximum peak height (µm)	4.17	49.29
R_z Maximum peak to valley height (µm)	8.13	112.72
R_{sk} Skewness of profile	0.16	−0.41

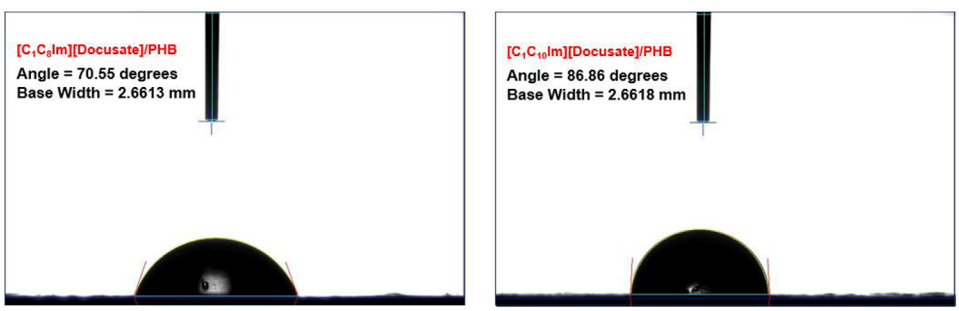

FIGURE 5 | Pictures relevant to static water contact angle measurements for $[C_1C_8Im][Docusate]$/PHB (left) and to $[C_1C_{10}Im][Docusate]$/PHB (right) membranes. Measurements were carried out in triplicate, with membranes, containing 60 wt.% of IL.

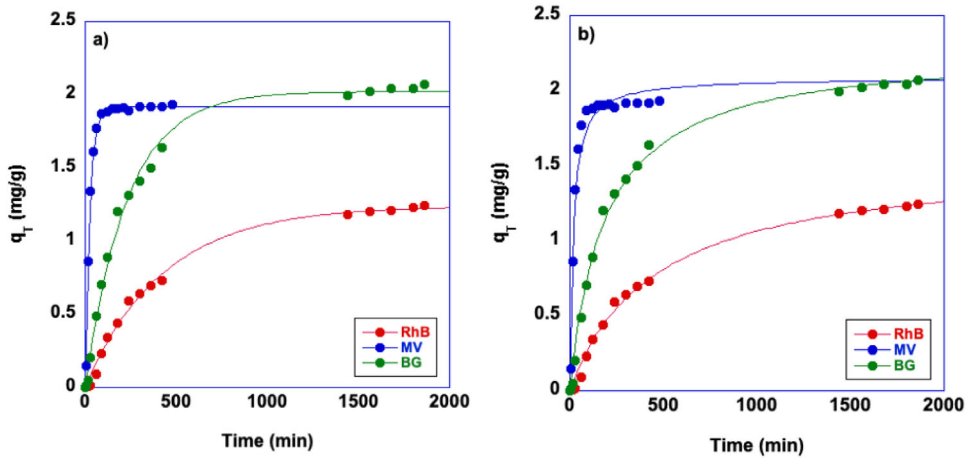

FIGURE 6 | Representative plots relevant to adsorption kinetic experiments, for $[C_1C_8Im][Docusate]$/PHB, fitted by (a) pseudo-first order and (b) pseudo-second order models. Content of IL = 60 wt.%, section 2 cm × 1 cm, $T = 25$ °C, 10 mL of dye solution 1×10^{-4} M.

solutions. To this purpose, we contacted sections of membranes as already described, for 4 h, at 25 °C, with aqueous solution of dyes with concentrations ranging from 5.0×10^{-5} M to 2.0×10^{-4} M, obtaining the removal efficiencies reported in Figure S5 and Table S3.

Perusal of the results reported in Figure S5 shows that, in general, both membranes keep their performance constant within the range of initial concentrations considered, except for the anionic dyes EY and MO. In these cases, in which both membranes have low affinity for these dyes, the magnitudes of RE%, regularly decrease on increasing the initial concentration, suggesting saturation of the membranes occurring already at the lowest dye concentration, 5×10^{-5} M.

Summarizing the evidences obtained in the optimization study, we found that in general, our membranes work better with cationic and neutral dye, compared to the anionic ones. The best performances were obtained using membranes doped with 60 wt.% of ILs, using a section exposed to the solution of size 2 cm × 1 cm. Therefore, we used these experimental conditions for all the experiments described in the following section.

2.4 | Adsorption Kinetics

To draw information about the rate of adsorption by the IL-doped membranes, we carried out kinetic tests, ran by determining adsorption capacity as a function of time. More specifically, these experiments were conducted by contacting 10 mL of 10^{-4} M dye solutions with sections (2 cm × 1 cm) of membrane, at 25 °C. We did not carry out kinetic tests in the presence of anionic dyes, given the low removal efficiency displayed by both hybrid membranes. Representative plots are reported in Figure 6, while the other ones are reported in Figures S6 and S7 and Table S4.

To gain insight on the rate of adsorption, we firstly fitted our results with by different model such as pseudo-first order [36], and the pseudo-second order model [37]. The equations describing each model, together with the meaning of the relevant parameters, are reported in the Supporting Information.

In most cases, the pseudo-first- and pseudo-second-order models gave good fits, with R^2 values close to unity as reported in Table S4. Given that comparing the values R^2 was undecisive, we based our assessment of model selection on further statistical parameters such as Akaike Information Criterion (AIC) [38] and Bayesian Information criterion (BIC) [39] which have been previously employed to elucidate adsorption kinetics models [40].

According to this criterion, a significantly lower value of AIC or BIC indicates the model that better describes the results. The values of AIC and BIC, obtained for pseudo-first- and pseudo-second-order models, reported in Table S4, allow us to draw some comments.

In general, we can observe different kinetic behaviors as a function of the dye. In particular, BG and BB (neutral dyes) exhibit pseudo-second-order kinetics in the presence of both membranes, whereas the uptake of MV and MB for both membranes follows a pseudo-first-order kinetics. Another different situation is found for RhB, in which case, the pseudo-first order is found in the presence of $[C_1C_{10}Im][Docusate]$/PHB and the pseudo-second order in the presence of $[C_1C_8Im][Docusate]$/PHB. Finding different kinetic law for adsorption on the same sorbent is rarely reported in the literature. For instance, a paper reported that adsorption of anionic and cationic dyes onto the same activated carbon sorbent followed different kinetic laws [41].

The values of the kinetic constants obtained by fitting the results with the respective kinetic models, as a function of the hybrid film, are reported in Figure 7.

Analyzing the results reported in Figure 7 shows that in two cases out of four, dyes adsorb faster onto the $[C_1C_{10}Im][Docusate]$/PHB membrane. Given that the difference between the two sorbents is constituted by the alkyl chain length of the ILs, this result hints at a certain relevance of van der Waals interactions between the IL embedded in the membrane and the organic dye, assisting the adsorption process. The exceptions are constituted by BG and MV. More specifically, for BG we found no significant difference as a function of the sorbent. Conversely, MV is the only dye in which adsorption occurs much faster onto $[C_1C_8Im][Docusate]$/PHB.

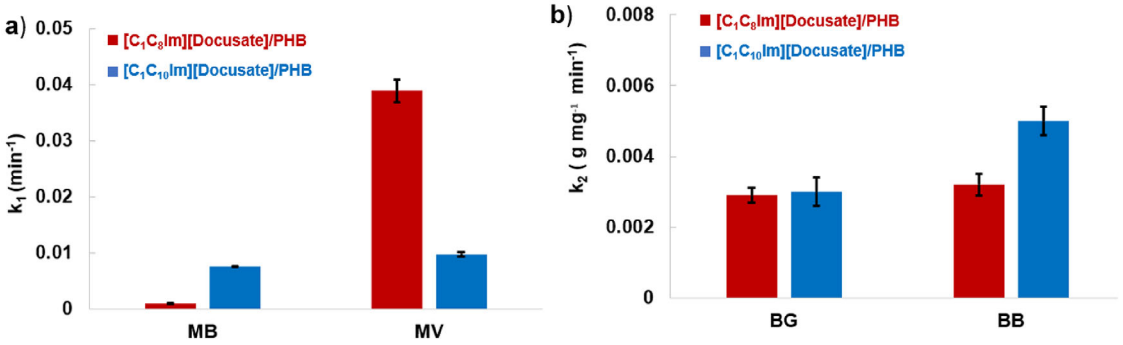

FIGURE 7 | Adsorption kinetic constants, found for dyes following (a) pseudo-first- and (b) pseudo-second-order kinetic laws. Content of IL = 60 wt.%, sections (2 cm × 1 cm), $T = 25\,^{\circ}C$, 10 mL of dye solution 1×10^{-4} M.

Obviously, a meaningful explanation of these findings requires comparison between dyes following the same kinetic law and with similar charges. In particular, among the neutral dyes, BB is characterized by a less polar substituent on the phenyl ring than BG (isopropyl vs. bromine). This is therefore consistent with the rate enhancement occurring for BB on going from $[C_1C_8Im][Docusate]$/PHB to $[C_1C_{10}Im][Docusate]$/PHB and not with BG, devoid of apolar moieties. Conversely, MV is sterically bulkier than MB. Hence, we hypothesize that the rate enhancement for MV in $[C_1C_8Im][Docusate]$/PHB can be due to steric factors. Indeed, steric factors have been shown in the literature to influence both adsorption thermodynamics and kinetics [42].

Finally, to evaluate the performance of our materials in the presence of mixtures of dyes, we conducted kinetic measurements, under the same experimental condition described, but with solutions containing both MB and BB. The choice of this couple of dyes is due to the necessity to avoid overlapping of adsorption peaks. The plots relevant to these kinetic tests are reported in Figure S8. Analysis of the results reported in Figure S8 hints at a synergistic effect occurring, since the pseudo-first-order kinetic constant increases on going from the single dye solutions to the binary mixture ($k_1 = 1.00 \times 10^{-3}$ and 3.3×10^{-2} min^{-1} for $[C_1C_8Im][Docusate]$/PHB; $k_1 = 1.1 \times 10^{-2}$ and 8.0×10^{-2} min^{-1} for $[C_1C_8Im][Docusate]$/PHB). This synergistic effect also influences the adsorption kinetics of BB, which now follows a pseudo-first-order kinetic trend.

2.5 | Adsorption Isotherms

To obtain information about the mechanism of adsorption by the membranes and to determine their maximum adsorption capacity, we conducted static adsorption experiments by varying the mass of sorbent and the volumes of solution. Each experiment was carried out for a suitable time, after which the amount of adsorbed dye did not change significantly, ensuring that equilibrium was reached. Representative plots of equilibrium adsorption capacity, q_e (mg/g) as a function of residual dye concentration in solution, C_e (mg/L), are reported in Figure 8, while the other ones are reported in Figure S9. It is worth noting that, due to the very limited extent of adsorption, we did not determine the adsorption isotherm in the presence of the anionic dyes, EY and MO. In addition, it was not possible to obtain an acceptable isotherm for MB, due to precipitation of the dye occurring at higher concentrations.

The plots of q_e as a function of C_e describe typical hyperbolic trends. To obtain mechanistic insights on the adsorption process, we fitted the curve according to two of the most widely accepted adsorption models, namely, the Langmuir and the Freundlich isotherms [43]. In particular, the Langmuir model assumes monolayer coverage of the adsorbate on the surface of the sorbent, which is treated as homogeneous and q_e is expressed by Equation (1):

$$q_e = \frac{K_L{}^* q\max{}^* C_e}{1 + K_L{}^* C_e} \quad (1)$$

where q_{max} is the maximum adsorption capacity and K_L is the Langmuir constant. On the other hand, the Freundlich model is based in multilayer adsorption, and treats the surface of the adsorbent as heterogeneous, with q_e expressed by Equation (2):

$$q_e = K_F{}^* (C_E)^{1/n} \quad (2)$$

where K_F is the Freundlich constant, related to the adsorption capacity and affinity of the sorbent toward the dye, and n is related to the adsorption intensity [44, 45]. The results of the nonlinear fitting based on the two models are summarized in Table 2.

Inspection of the results reported in Table 2 shows that the adsorption process is, in all cases, best described by the Langmuir model, suggesting monolayer adsorption on the membrane surface, with the only exception of RhB, for which both models can successfully account for the adsorption outcome. Hence, for a meaningful comparison, we report the values of the maximum adsorption capacity q_{max}, for both membranes in Figure 9.

The results reported in Figure 9 confirm the findings of the preliminary adsorption tests, with both membranes showing the highest efficiency with the cationic dye MV. In addition, regardless of the dye considered, the $[C_1C_{10}Im][Docusate]$/PHB showed higher adsorption ability compared with $[C_1C_8Im][Docusate]$/PHB. The higher affinity of neutral dyes toward $[C_1C_{10}Im][Docusate]$/PHB, can be once again explained with the higher importance of van der Waals interactions on assisting the adsorption process, which makes

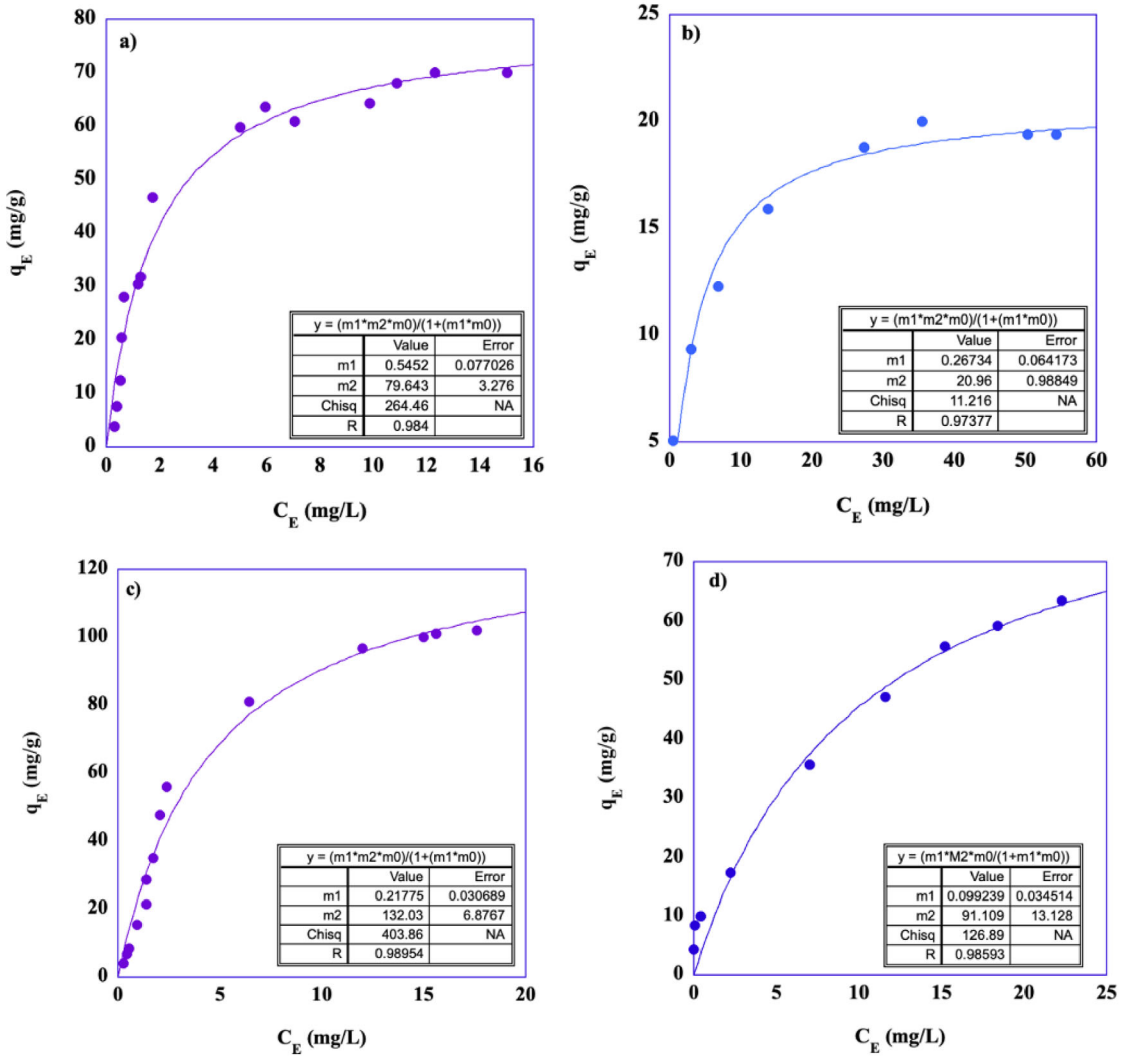

FIGURE 8 | Plots of adsorption isotherms for (a) [C_1C_8Im][Docusate]/PHB in the presence of MV, (b) [C_1C_8Im][Docusate]/PHB in the presence of BB, (c) [C_1C_{10}Im][Docusate]/PHB in the presence of MV, and (d) [C_1C_{10}Im][Docusate]/PHB in the presence of BB. Fitting of curves according to Langmuir model. Content of IL = 60 wt.%, sections (2 cm × 1 cm), $T = 25\,^{\circ}C$.

TABLE 2 | Results of nonlinear fitting according to mono- and multilayer adsorption models for [C_1C_8Im][Docusate]/PHB and [C_1C_{10}Im][Docusate]/PHB in contact with of different dye solutions.[a)]

[C_1C_8Im][Docusate]/PHB						
	q_{max} (mg/g)	K_L	R^2	K_F (L/g)	n	R^2
RhB	12.8 ± 0.3	0.078 ± 0.006	0.989	2.4±0.1	2.62±0.08	0.994
BG	51 ± 2	0.025 ± 0.003	0.989	3.3±0.5	1.8±0.1	0.969
MV	80 ± 3	0.54 ± 0.07	0.968	27 ± 3	2.6 ± 0.3	0.900
BB	21 ± 1	0.26 ± 0.06	0.946	7.5 ± 0.7	3.9 ± 0.4	0.925
[C_1C_{10}Im][Docusate]/PHB						
	q_{max} (mg/g)	K_L	R^2	K_F (L/g)	n	R^2
RhB	20 ± 2	0.020 ± 0.003	0.979	0.8 ± 0.1	1.5 ± 0.1	0.967
BG	89 ± 6	0.031± 0.005	0.987	5.1 ± 0.9	1.7 ± 0.1	0.974
MV	132 ± 7	0.22 ± 0.03	0.980	26 ± 3	1.9 ± 0.2	0.938
BB	90 ± 13	0.10 ± 0.03	0.977	14 ± 1	2.1 ± 0.2	0.980

[a)]content of IL = 60 wt.%. Sections (2 cm × 1 cm), $T = 25\,^{\circ}C$.

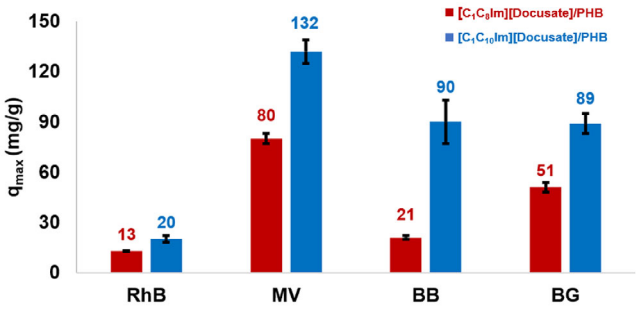

FIGURE 9 | Plot of q_{max} for adsorption of dyes on $[C_1C_8Im][Docusate]$/PHB and $[C_1C_{10}Im][Docusate]$/PHB. Content of IL = 60 wt.%, sections (2 cm × 1 cm), $T = 25\,^{\circ}C$.

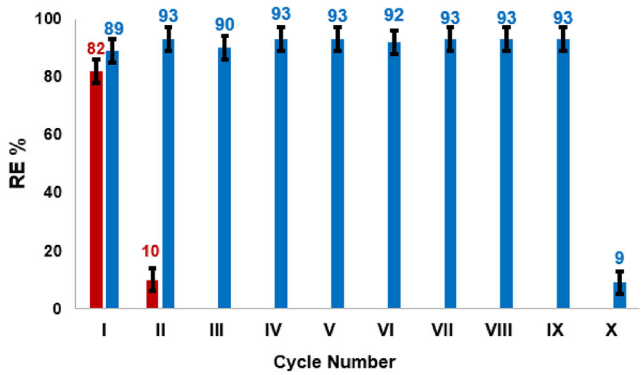

FIGURE 10 | Plots of removal efficiencies after 4 h for MB upon reusing $[C_1C_8Im][Docusate]$/PHB (red) and $[C_1C_{10}Im][Docusate]$/PHB membranes (blue). Content of IL = 60 wt.%, sections (2 cm × 1 cm), 1×10^{-4} M 10 mL of 1×10^{-4} M dye solution. Measurements were carried out in triplicate and RE% are reproducible within ± 3%.

this system not only the most efficient sorbent, but also the one which in most cases, gives rise to the fastest adsorption.

To better understand if the influence of interfering ions, we carried out, as a representative case, the adsorption of MB from NaCl or KCl 0.5 M solution as well as a solution with the same ionic strength but containing a divalent anion, that is, Na_2SO_4 0.17 M, obtaining the results reported in Figure S10, expressed in terms of q/q_0, where q is the adsorption capacity observed in the presence of the interferent, while q_0 is the adsorption capacity obtained in water. Perusal of the results reported in Figure S10, shows that in both cases, the presence of the Na^+ cation induces a distinct decrease in adsorption capacity, in the case of $[C_1C_{10}Im][Docusate]$/PHB, with q/q_0 equal to 0.37 and 0.28 in the presence of Na_2SO_4 and NaCl, respectively, while in the presence of KCl it is close to unity, that is, 0.92.

In general, the performance of $[C_1C_8Im][Docusate]$/PHB appears more tolerant of the presence of interfering ions, with q/q_0 equal to 0.92 with Na_2SO_4 and KCl, respectively, while it decreases to 0.56 in the presence of NaCl. Such results suggest that the sodium cation competes more efficiently for the adsorption sites. Together with efficiency and rate, in adsorption processes, a desirable feature of any sorbent system is the possibility of reusing, particularly when no intermediate washing and regeneration step are required in between each adsorption runs. This allows reducing the amount of materials employed in the process, and, consequently, the amount of pollutant-laden membrane produced at the end.

To illustrate the extent of reuse of our membranes, we chose the cationic dye MB. To this aim, for both membranes we carried out static adsorption runs, under the same experimental conditions already described. Then, after determining the RE%, the supernatant was removed and replaced with a fresh batch of dye solution. The results obtained are displayed in Figure 10.

The plot reported in Figure 10 reveals a markedly different behavior of the two membranes, with the $[C_1C_8Im][Docusate]$/PHB that is practically non-recyclable, due to saturation of the materials already at the first cycle. Conversely, the $[C_1C_{10}Im][Docusate]$/PHB membrane maintains its removal efficiency for nine reuses, after which the removal efficiency abruptly plummets to 9%, due to saturation of the active sites.

2.6 | Comparison with Literature Systems

To better evaluate the performance of our materials, we report below a comparison between the best-performing membrane, $[C_1C_{10}Im][Docusate]$/PHB, with similar systems available in the literature for the adsorption of dyes. It is important to note that we limit our discussion to works providing the maximum adsorption capacity values (q_{max}), and not only RE%, for a meaningful comparison. Furthermore, we compare the values obtained for a cationic dye, MV and a neutral one, BG, to have information about the performance of our system in the presence of dyes of different classes. The results are reported in Table 3.

Looking at the results reported in Table 3 shows that the performance of our material is higher or full in line with most of similar membrane-based systems reported in the literature. In particular, despite the simple preparation, the adsorption capacity of $[C_1C_{10}Im][Docusate]$/PHB for MV is comparable with the ones of a cellulose-based membrane [48] and MOF-doped membrane [49] toward cationic dyes as MB or crystal violet (entries 1, 5, and 6), while it is significantly higher compared with a polyethylene-based membrane (entries 1 and 4). On the other hand, a cross-linked IL polymer [50], reported by Reddy et al., outperforms our materials, although with a lower degree of reusability, given that it was reused for three times as opposed to $[C_1C_{10}Im][Docusate]$/PHB, which could be reused for nine cycles with the same dye.

In addition, our material shows a significantly higher values of q_{max} for BB, compared with a chitosan/polymethacrylate composite [46] for the same dye (entries 2 and 3).

2.7 | Photocatalytic Tests

With the aim to reduce the amount of polluted material generated at the end of the adsorption process, we verified the possibility to degrade organic dyes directly in the same aqueous phase. To this purpose, the best performing system, $[C_1C_{10}Im][Docusate]$/PHB, was coupled with TiO_2 nanoparticles to obtain hybrid nanocomposites. The polymeric part was used as a support, while the

TABLE 3 | Comparison of q_{max} values of for $[C_1C_{10}Im][Docusate]$/PHB and membrane-based systems previously reported in literature.

Entry	Sorbent	Dye	q_{max} (mg/g)
1	$[C_1C_{10}Im][Docusate]$/PHB [a)]	MV	132
2	$[C_1C_{10}Im][Docusate]$/PHB [a)]	BG	89
3	Chitosan/poly(methacrylate) composite [46]	BG	40
4	Polyethylene-based membrane [47]	MB	43
5	Cellulose-based membrane [48]	MB	126
6	MOF-doped membrane [49]	Crystal violet	157
7	Cross-linked ionic liquid polymer [50]	MB	1212

[a)]This work.

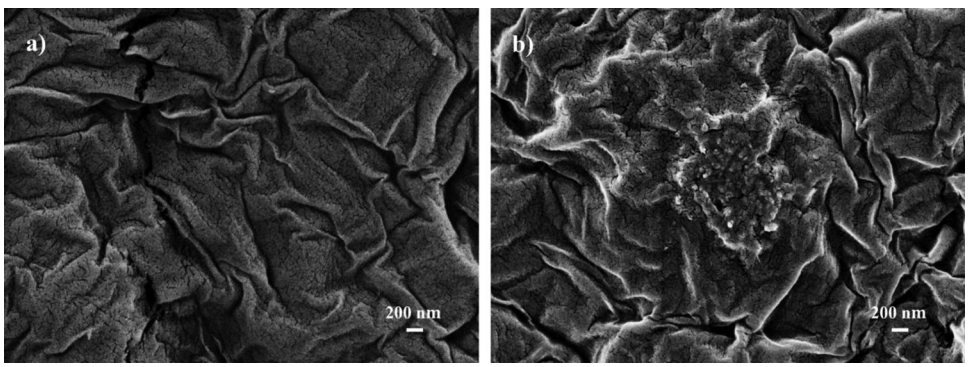

FIGURE 11 | Plan-view SEM images of (a) $[C_1C_{10}Im][Docusate]$/PHB and (b) $[C_1C_{10}Im][Docusate]$/PHB/TiO_2 membranes at magnifications of 50.000×. Both samples were sputter-coated with a thin Au layer to avoid surface charging during the SEM analyses. Content of IL = 60 wt.%, content of TiO_2 = 5 wt.%.

TiO_2 was used for its widely studied photocatalytic properties. In particular, the membranes were prepared by incorporating 5 wt.% of commercial TiO_2.

The SEM images in plan-view of both the membranes, namely, $[C_1C_{10}Im][Docusate]$/PHB and $[C_1C_{10}Im][Docusate]$/PHB/TiO_2, are reported in Figures 11 and S11, to evaluate if any change in morphology occurred upon incorporation of TiO_2 on the membrane surfaces.

A comparison of the images reported in Figure 11 clearly shows the presence of aggregates of TiO_2 nanoparticles, in agreement with the seller's specifications. In particular, as shown in Figure S12, at lower magnification, it is possible to observe a non-uniform distribution of these aggregates over the surface. However, the inclusion of TiO_2 preserves the integrity of the membrane surface morphology; indeed, the surface structure of the two samples remains the same. The distribution of the photocatalyst within the thickness of the membranes was further examined through cross-sectional SEM analyses. As shown in Figure S12, the amount of TiO_2 progressively decreases along the cross-section, with the nanoparticles being primarily concentrated at the bottom of the membrane (i.e., the membrane side in contact with the Petri dishes).

The photocatalytic performance of the hybrid membranes was initially evaluated through the degradation of RhB dye. Prior to the photocatalytic test, the adsorption capacity of the samples was assessed by monitoring the adsorption of RhB onto their surfaces. Once the adsorption equilibrium was reached, the photocatalytic experiment was performed as detailed in Supporting Information.

Figure 12 shows C/C_0 as a function of time t, where C is the concentration of the RhB in the aqueous solution at time t, C_0 is the starting concentration of the dye (i.e., 1.5×10^{-5} M).

The investigated samples checked were: $[C_1C_{10}Im][Docusate]$/PHB membrane (green squares) and $[C_1C_{10}Im][Docusate]$/PHB/TiO_2 (orange squares); a solution of RhB alone was also checked as a reference (magenta squares).

The RhB was not degraded in the absence of any samples (magenta squares), as expected; indeed, its concentration remained constant. The polymeric membranes without TiO_2 (green squares) surprisingly showed a slight degradation of the RhB dye. Although the PHB was a non-conductive polymer and thus lacks a conventional electron transfer mechanism typical of semiconductors, it can still promote minor degradation through UV-induced photodegradation processes. The UV irradiation provides sufficient energy to break the C–C bonds of the polymer chain, generating polymeric radicals on the material's surface. These radicals react with oxygen, initiating a chain of reactions that lead to the formation of highly reactive oxidizing species, such as hydroxyl radicals. These oxidizing species can attack and degrade pollutant molecules adsorbed at the PHB surface, in a analogous manner to traditional photocatalytic processes using

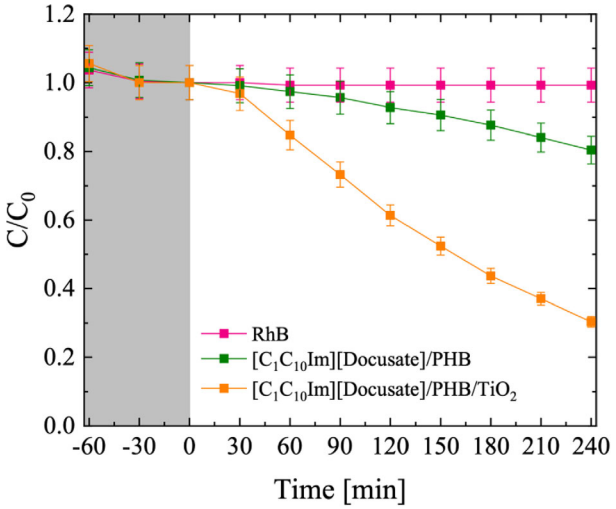

FIGURE 12 | Photodegradation of RhB as a function of irradiation time for $[C_1C_{10}Im][Docusate]/PHB$ (green squares), $[C_1C_{10}Im][Docusate]/PHB/TiO_2$ (orange squares), and pure RhB as control (magenta squares). Content of IL = 60 wt.%, content of TiO_2 = 5 wt.%, section 1 cm^2, 2 mL of dye solution 1.5×10^{-5} M.

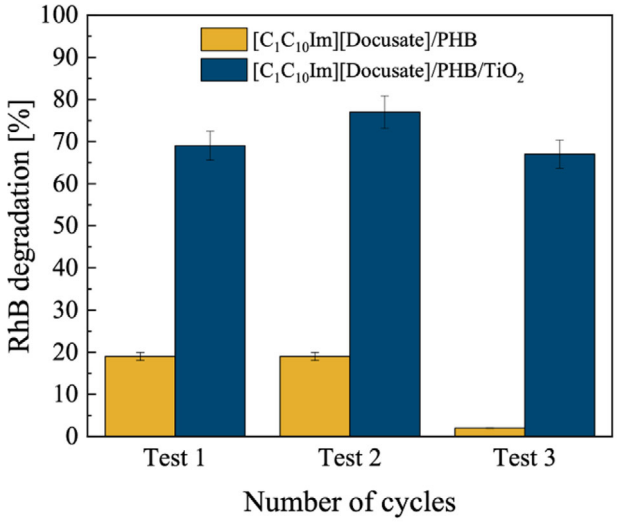

FIGURE 13 | RhB degradation (%) after 4 h UV-light irradiation for $[C_1C_{10}Im][Docusate]/PHB$ and $[C_1C_{10}Im][Docusate]/PHB/TiO_2$, during the first photocatalytic test (Test 1), the second photocatalytic test (Test 2), and the third photocatalytic test (Test 3). Content of IL = 60 wt.%, content of TiO_2 = 5 wt.%, T = 25 °C.

inorganic semiconductors [51]. In the presence of the membrane containing TiO_2 (orange squares), with the bottom side exposed, the RhB concentration decreased significantly over the time. To quantitatively evaluate the photocatalytic efficiency of the samples, the degradation rate constant was calculated using the Langmuir–Hinshelwood model. This model assumes a first-order degradation mechanism for the pollutant [52], described by the following equation:

$$\ln \frac{C}{C_0} = -kt \tag{3}$$

where k is the pseudo-first-order rate constant, C is the RhB concentration at the time t, and C_0 is the initial RhB concentration. In detail, the kinetic constant was estimated to be $(5.4 \pm 0.3) \times 10^{-3}$ min^{-1} for the $[C_1C_{10}Im][Docusate]/PHB/TiO_2$ membranes, versus $(1.1 \pm 0.1) \times 10^{-3}$ min^{-1} for the $[C_1C_{10}Im][Docusate]/PHB$ reference samples. The obtained results indicate that the membrane containing 5 wt.% TiO_2 exhibited excellent photocatalytic properties, as it effectively degrades the RhB previously adsorbed on its surface.

To confirm the hypothesis that the bottom side exhibits superior photocatalytic performance due to a higher concentration of TiO_2 nanoparticles (the reader can refer to Figure S12), a photodegradation experiment with RhB was carried out using two $[C_1C_{10}Im][Docusate]/PHB/TiO_2$ membranes, exposing either the bottom side (i.e., the side in contact with the Petri dishes) or the top side (i.e., the side in contact with the air) of the material to UV-light. The comparison of their performances was shown in Figure S13. In particular, the sample exposing the bottom side exhibited the highest degradation efficiency. This is further confirmed by the obtained degradation rate constants, which are $(5.4 \pm 0.3) \times 10^{-3}$ min^{-1} for the membrane with TiO_2 exposing the bottom side, versus $(4.2 \pm 0.2) \times 10^{-3}$ min^{-1} for the membrane with TiO_2 exposing the top side. Since the bottom side performed better than the top, all tests were correctly conducted with the bottom side facing UV-light.

To evaluate the stability and reusability of the films, two additional adsorption–photodegradation tests were performed without bleaching the material at the end of each test. This means that the solution used in the previous test was removed, and the wells were refilled with a fresh RhB solution at a concentration of 1.5×10^{-5} M, without any cleaning of the composites. The results of the second and third photocatalytic tests (Test 2 and Test 3) are reported in Figure 13, in comparison with the first test (Test 1). Figure 13 shows that RhB degradation capacity (expressed as %) of the $[C_1C_{10}Im][Docusate]/PHB/TiO_2$ nanocomposites is comparable within the experimental error for the three different tests. Indeed, the membranes show similar degradation percentages across the three tests: 70% in Test 1, 75% in Test 2, and 65% in Test 3. This confirms that the photocatalytic properties of the membranes containing 5 wt.% TiO_2 are maintained, demonstrating the stability of the materials. Another observation concerns the slight degradation of the dye induced by the membrane without TiO_2 also in the second photocatalytic test (Test 2), which is not observed in the third photocatalytic test (Test 3). This suggests that the marginal photoinduced activity associated with the polymer surface diminishes upon repeated irradiation, becoming practically irrelevant after multiple reuse cycles. Similar trends have been reported in the literature, where the surface reactivity of PHB under UV exposure progressively decreases with cycling [51].

To demonstrate that the hybrid membranes are active in the degradation of another water pollutant, the photocatalytic properties of the materials were evaluated for the photodegradation of the MB (another cationic dye). The adsorption capacity of the samples was evaluated by monitoring the adsorption of MB onto their surfaces in the dark, until the equilibrium was reached. Once the adsorption equilibrium was achieved,

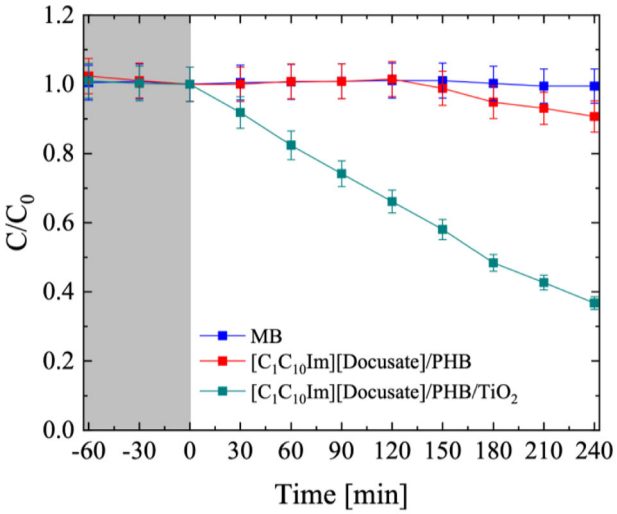

FIGURE 14 | Photodegradation of MB as a function of the irradiation time for $[C_1C_{10}Im][Docusate]/PHB$ (red squares), $[C_1C_{10}Im][Docusate]/PHB/TiO_2$ (teal squares), and pure MB as control (blue squares). Content of IL = 60 wt.%, content of TiO_2 = 5 wt.%, T = 25 °C.

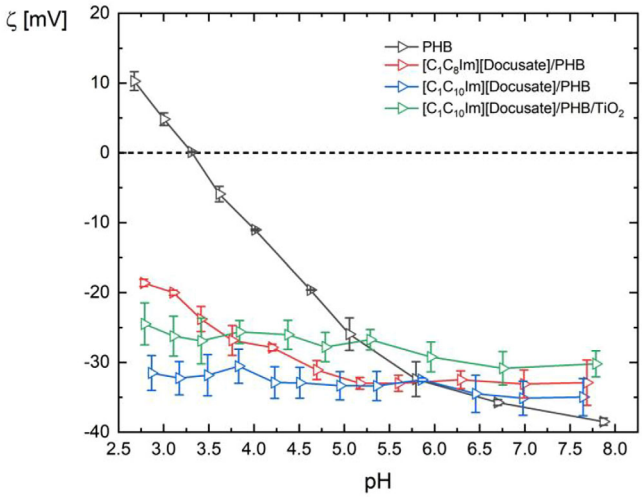

FIGURE 15 | Plot of ζ-potential as a function of pH for PHB, $[C_1C_8Im][Docusate]/PHB$, $[C_1C_{10}Im][Docusate]/PHB$, and $[C_1C_{10}Im][Docusate]/PHB/TiO_2$. Content of IL = 60 wt.%, content of TiO_2 = 5 wt.%, T = 25 °C. Lines are drawn as mere visual guides.

the solution in contact with the hybrid membranes was replaced with a fresh dye solution at a concentration of 1.5×10^{-5} M for the photocatalysis test (Figure 14). The investigated samples were: $[C_1C_{10}Im][Docusate]/PHB$ (red squares), $[C_1C_{10}Im][Docusate]/PHB/TiO_2$ (teal squares); a solution of MB alone was also checked as a reference (blue squares).

Similarly to what was observed in the RhB test (Figure 12), MB was not degraded in the absence of any samples. In contrast, in the presence of the membrane containing TiO_2, the MB concentration decreased significantly over time, as also confirmed by the calculated degradation rate constants: $(4.2 \pm 0.2) \times 10^{-3}$ min^{-1} for the $[C_1C_{10}Im][Docusate]/PHB/TiO_2$ membrane, $(9.2 \pm 0.5) \times 10^{-4}$ min^{-1} for the $[C_1C_{10}Im][Docusate]/PHB$ reference sample. For the same reasons discussed previously for the RhB photodegradation (Figure 12), the pure PHB membrane also induced a slight degradation of MB.

The results obtained with RhB and subsequently with MB confirm that the polymeric film nanocomposites incorporating 5 wt.% of TiO_2 P25 nanoparticles exhibit excellent photocatalytic properties for the degradation of cationic dyes in aqueous solution.

Finally, another important property of the surface of sorbent materials is their ζ-potential. Consequently, to gain information on such properties, we have measured the ζ-potential as a function of pH for the pristine PHB film, both IL-doped membranes, $[C_1C_8Im][Docusate]/PHB$ and $[C_1C_{10}Im][Docusate]/PHB$, as well as the hybrid membrane $[C_1C_{10}Im][Docusate]/PHB/TiO_2$, obtaining the results reported in Figure 15 and Table S5.

Analysis of the plot reported in Figure 15 shows a descending trend for the pristine PHB film surface on increasing pH. The ζ-potential values decrease from +10 to −38 mV, as pH increases from 2.5 to 8, with an isoelectric point of 3.5. This is consistent with the presence of acidic group on the polymer surface, that is, the terminal carboxylic acid groups, which are deprotonated as pH exceeds their pKa. Conversely, all the IL-doped membranes maintain consistent, stable negative values of ζ-potential through the whole pH-range considered, due to the presence of permanently ionized sulfonate groups form the docusate anions. This suggests high stability of the membrane surface regardless of pH of the aqueous environment in which they are placed. The rather flat appearance of the curve also hints at uniformly distributed IL within the surface. The negative values of the ζ-potential are also consistent with the high adsorption ability of the membranes toward cationic dyes, rather than anionic. Similar conclusions hold true for the hybrid membrane $[C_1C_{10}Im][Docusate]/PHB/TiO_2$.

3 | Conclusions

In this work, we prepared and characterized IL-doped membranes based on the bio-derived polymer PHB, namely, $[C_1C_8Im][Docusate]/PHB$ and $[C_1C_{10}Im][Docusate]/PHB$, employing them as sorbents to remove dyes from aqueous solution. The ILs comprised imidazolium cations and the hydrophobic docusate anion, well-known for its ability to give low toxic salts, and differed for the alkyl chain length. This latter affects hydrophobicity and relevance of van der Waals interactions, which in turn can significantly influence the adsorption process.

The preparation of the materials was straightforward, with no synthetic or purification steps required, and the membranes obtained were characterized in terms of morphology, surface roughness and water contact angle, which showed their hydrophobic character. Subsequently, we studied the ability of such materials to act as sorbents for the removal of different dyes from aqueous phases, considering either cationic, anionic or neutral dyes. The adsorption process was studied in terms of adsorption kinetics finding that adsorption rate could

be described by both pseudo-first and pseudo-second models, depending on the dye.

Adsorption isotherms suggested monolayer adsorption, according to the Langmuir model. Both membranes exhibited selectivity toward neutral and cationic dyes over anionic ones, and the [C_1C_{10}Im][Docusate]/PHB membrane showed larger adsorption capacity than [C_1C_8Im][Docusate]/PHB, achieving the highest values for MV and BB, equal to 132 and 90 mg/g, respectively. In general, van der Waals interactions were hypothesized to exert a significant effect on the affinity between surface and adsorbates. The same membrane could be reused nine times without significant loss in efficiency or need for intermediate washing, overall showing a performance superior or comparable to most related systems reported in the literature. Finally, to reduce the environmental impact of the adsorption process, we evaluated the possibility to directly degrade the pollutants in the same aqueous phase. To this aim, we further doped the best-performing membrane with a photocatalyst like TiO_2, which enabled almost thorough and fast photodegradation of cationic dyes like RhB and MB. Such photocatalyst also showed a good degree of recyclability and could be reused three times with no loss in efficiency and without intermediate bleaching. Therefore, in our view, the present system uses a safe, bio-derived polymer source to obtain, in a straightforward way, an effective and recyclable sorbent for dyes, with no need for intermediate washing, which, suitably doped with TiO_2, provide also an efficient and recyclable photocatalyst, to degrade dyes in solution. The systems herein investigated could provide a useful tool to reuse spent PHB, ultimately reducing the costs deriving from its production.

4 | Experimental Section

4.1 | Materials

Poly-(3-hydroxybutirate), 1-decyl-3-methylimidazolium chloride, 1-octyl-3-methylimidazolium chloride, sodium docusate, chloroform, methanol, methylene blue, rhodamine B, eosin yellow, methyl violet, bromocresol green, chloroform, and dichloromethane were obtained from commercial sources and used without further purification. ILs, [C_1C_8Im][docusate] and [C_1C_{10}Im][docusate], were prepared by metathesis from the relevant chlorides and sodium docusate, following a published procedure [53].

Commercial TiO_2 P25 (3-99 nm particle size) was purchased from Evonik (Essen, Germany).

Other experimental details are reported in the Supporting Information.

4.2 | 1-Decyl-3-methylimidazolium docusate [C1C10Im][docusate]

Pale yellow oil. Yield: 79%. ^{1}H-NMR (400 MHz, $CDCl_3$) δ: 9.55 (s, 1H), 7.43 (t, J = 4.0 Hz, 1H), 7.28 (t, J = 4.0 Hz, 1H), 4.22 (t, J = 8.0 Hz, 2H), 4.02 (m, 2H), 3.99 (s, 3H), 3.96 (m, 2H), 3.17 (m, 2H), 1.87 (m, 3H), 1.57 (m, 2H), 1.24 (m, 29H), 0.86 (m, 14H). ^{13}C-NMR (400 MHz, $CDCl_3$) δ: 171.57, 169.29, 123.56, 121.37, 67.63, 67.56, 67.05, 62.33, 49.94, 30.26, 29.43, 29.36, 29.21, 29.00 (2C, overlapped), 28.84, 22.91, 22.60, 14.04, 14.00, 10.91, 10.86, 10.81 ppm.

4.3 | 1-Octyl-3-methylimidazolium docusate [C_1C_8Im][docusate]

Pale yellow oil. Yield: 79%. ^{1}H-NMR (400 MHz, $CDCl_3$) δ: 9.57 (s, 1H), 7.42 (t, J = 4.0 Hz, 1H), 7.28 (t, J = 4.0 Hz, 1H), 4.22 (t, J = 8.0 Hz, 2H), 4.14 (dd, J_1 = 8.0 Hz, J_2 = 4.0 Hz, 1H), 4.03 (m, 2H), 3.99 (s, 3H), 3.94 (m, 2H), 3.17 (m, 2H), 1.85 (m, 4H), 1.25 (m, 26H), 0.86 (m, 15H). ^{13}CNMR (400 MHz, $CDCl_3$) δ: 171.57, 169.00, 137.88, 123.87, 122.02, 67.04, 61.98, 50.08, 31.64, 30.25, 29.00, 28.93, 28.83, 26.21, 22.90, 22.53, 13.99, 10.90, 10.86, 10.73 ppm.

Author Contributions

Salvatore Marullo: Writing – original draft, Writing – review and editing, visualization; **Luigi Cino**: investigation: material preparation and adsorption experiments; **Chiara Laferrera**: investigation; photocatalysis experiments, writing – original draft; **Vincenzo M. Marzullo**: investigation, ζ-potential measurements; **Giuliana Impellizzeri**: supervision, writing – original draft, writing – review and editing, conceptualization, funding acquisition; **Francesca D'Anna**: conceptualization, writing – review and editing, supervision and funding acquisition.

Acknowledgements

The authors thank MUR for funding, SiciliAn MicronanOTecH Research And Innovation CEnter "SAMOTHRACE" (MUR, PNRR-M4C2, ECS_00000022), spoke 3 and spoke 4. Università degli Studi di Palermo "S2-COMMs–Micro and Nanotechnologies for Smart & Sustainable Communities." The funding source had no role in analysis, design, interpretation of results, and report writing. SEM images in Figure 3 and water contact angle measurements were acquired at ATeN Center of University of Palermo—Laboratorio di Preparazione e Analisi di Biomateriali. Surface roughness measurements were acquired at ATeN Center of University of Palermo- Laboratorio di Meccanica dei Materiali e dei BioMateriali.

Conflicts of Interest

The authors declare no conflict of interest.

Data Availability Statement

The data that supports the findings of this study are available in the supplementary material of this article.

References

1. R. S. Dhamorikar, V. G. Lade, P. V. Kewalramani, and A. B. Bindwal, "Review on Integrated Advanced Oxidation Processes for Water and Wastewater Treatment," *Journal of Industrial and Engineering Chemistry* 138 (2024): 104–122, https://doi.org/10.1016/j.jiec.2024.04.037.

2. E. Mansor, H. Abdallah, and A. M. Shaban, "The Role of Membrane Filtration in Wastewater Treatment," *Environmental Quality Management* 34 (2024): 22251, https://doi.org/10.1002/tqem.22251.

3. D. Singh, D. Singh, V. Mishra, et al., "Strategies for Biological Treatment of Waste Water: A Critical Review," *Journal of Cleaner Production* 454 (2024): 142266, https://doi.org/10.1016/j.jclepro.2024.142266.

4. R. Rashid, I. Shafiq, P. Akhter, M. J. Iqbal, and M. Hussain, "A State-of-the-Art Review on Wastewater Treatment Techniques: The Effectiveness

of Adsorption Method," *Environmental Science and Pollution Research* 28 (2021): 9050–9066, https://doi.org/10.1007/s11356-021-12395-x.

5. H. Alkhaldi, S. Alharthi, S. Alharthi, et al., "Sustainable Polymeric Adsorbents for Adsorption-Based Water Remediation and Pathogen Deactivation: A Review," *RSC Advances* 14 (2024): 33143–33190, https://doi.org/10.1039/D4RA05269B.

6. Y. Wang, Y. Guo, C. Yang, et al., "Bio-inspired Fabrication of Adsorptive Ultrafiltration Membrane for Water Purification: Simultaneous Removal of Natural Organic Matters, Lead Ion and Organic Dyes," *Journal of Environmental Chemical Engineering* 11 (2023): 109798–109798, https://doi.org/10.1016/j.jece.2023.109798.

7. Z. Q. Huang and Z. F. Cheng, "Recent Advances in Adsorptive Membranes for Removal of Harmful Cations," *Journal of Applied Polymer Science* 137 (2020): 48579–48579, https://doi.org/10.1002/app.48579.

8. K. C. Khulbe and T. Matsuura, "Removal of Heavy Metals and Pollutants by Membrane Adsorption Techniques," *Applied Water Science* 8 (2018): 19–19, https://doi.org/10.1007/s13201-018-0661-6.

9. M. R. Adam, M. H. D. Othman, T. A. Kurniawan, et al., "Advances in Adsorptive Membrane Technology for Water Treatment and Resource Recovery Applications: A Critical Review," *Journal of Environmental Chemical Engineering* 10 (2022): 107633–107633, https://doi.org/10.1016/j.jece.2022.107633.

10. H. Wan, X. Zhu, J. Wang, et al., "Adsorptive Nanofibrous Membranes for Bidirectional Removal of Cationic and Anionic Dyes," *Separation and Purification Technology* 361 (2025): 131515, https://doi.org/10.1016/j.seppur.2025.131515.

11. J. Lin, Z. Yu, T. Chen, et al., "Sub-4 Nanometer Porous Membrane Enables Highly Efficient Electrodialytic Fractionation of Dyes and Inorganic Salts," *Nature Communications* 16 (2025): 3671, https://doi.org/10.1038/s41467-025-58873-5.

12. A. Torre-Celeizabal, F. Russo, F. Galiano, A. Figoli, C. Casado-Coterillo, and A. Garea, "Green Synthesis of Cellulose Acetate Mixed Matrix Membranes: Structure–Function Characterization," *ACS Sustainable Chemistry & Engineering* 13 (2025): 1253–1270.

13. S. Santana-Luna, M. Yam-Cervantes, R. Sulub-Sulub, et al., "Sustainable Membranes for Water Treatment from Expanded Polystyrene Waste Using Dimethyl Isosorbide as a Green Solvent," *ACS Sustainable Chemistry & Engineering* 13 (2025): 17939–17948, https://doi.org/10.1021/acssuschemeng.5c06312.

14. S. Divya, T. H. Oh, S. Divya, and T. H. Oh, "Polymer Nanocomposite Membrane for Wastewater Treatment: A Critical Review," *Polymers* 14 (2022): 1732, https://doi.org/10.3390/POLYM14091732.

15. M. Santhamoorthy, P. Asaithambi, I. Perumal, et al., "A Comprehensive Review of the Functionalized Polymer Composite Membranes in Wastewater Treatment," *Journal of Environmental Chemical Engineering* 13 (2025): 117735–117735, https://doi.org/10.1016/j.jece.2025.117735.

16. T. Welton, "Ionic Liquids: A Brief History," *Biophysical Reviews* 10 (2018): 691–706, https://doi.org/10.1007/s12551-018-0419-2.

17. J. P. Hallett and T. Welton, "Room-Temperature Ionic Liquids: Solvents for Synthesis and Catalysis," *Chemical Reviews* 111 (2011): 3508–3576, https://doi.org/10.1021/cr1003248.

18. K. Fatyeyeva, S. Rogalsky, S. Makhno, et al., "Polyimide/Ionic Liquid Composite Membranes for Middle and High Temperature Fuel Cell Application: Water Sorption Behavior and Proton Conductivity," *Membranes* 10 (2020): 82, https://doi.org/10.3390/MEMBRANES10050082.

19. A. Hernández-Fernández, E. Iniesta-López, A. Ginestá-Anzola, et al., "Polymeric Inclusion Membranes Based on Ionic Liquids for Selective Separation of Metal Ions," *Membranes* 13 (2023): 795, https://doi.org/10.3390/MEMBRANES13090795.

20. Y. Sutar, S. R. Fulton, S. Paul, et al., "Docusate-Based Ionic Liquids of Anthelmintic Benzimidazoles Show Improved Pharmaceutical Processability, Lipid Solubility, and in Vitro Activity against Cryptococcus Neoformans," *ACS Infectious Diseases* 7 (2021): 2637–2649, https://doi.org/10.1021/acsinfecdis.1c00063.

21. R. Sirohi, J. Prakash Pandey, V. Kumar Gaur, E. Gnansounou, and R. Sindhu, "Critical Overview of Biomass Feedstocks as Sustainable Substrates for the Production of Polyhydroxybutyrate (PHB)," *Bioresource Technology* 311 (2020): 123536, https://doi.org/10.1016/j.biortech.2020.123536.

22. J. C. C. Yeo, J. K. Muiruri, W. Thitsartarn, Z. Li, and C. He, "Recent Advances in the Development of Biodegradable PHB-based Toughening Materials: Approaches, Advantages and Applications," *Materials Science and Engineering: C* 92 (2018): 1092–1116, https://doi.org/10.1016/j.msec.2017.11.006.

23. M. Li, Y. Zhang, Y. Wang, et al., "Biodegradable Konjac Glucomannan-based Heat-resistant Fibrous Film for Teabag Applications," *Colloids and Surfaces A: Physicochemical and Engineering Aspects* 730 (2026): 138973, https://doi.org/10.1016/j.colsurfa.2025.138973.

24. M. Khoroushi, M. R. Foroughi, S. Karbasi, B. Hashemibeni, and A. A. Khademi, "Effect of Polyhydroxybutyrate/Chitosan/Bioglass Nanofiber Scaffold on Proliferation and Differentiation of Stem Cells from human Exfoliated Deciduous Teeth into Odontoblast-Like Cells," *Materials Science and Engineering: C* 89 (2018): 128–139, https://doi.org/10.1016/j.msec.2018.03.028.

25. B. M. Dakshinamoorthi, U. A. Chinnarasu Ananth, N. Krishnan, and S. Jothiraman, "Polyhydroxybutyrates: A Sustainable Alternative for Synthetic Polymers," *Biosciences Biotechnology Research Asia* 21 (2024): 851–862, https://doi.org/10.13005/bbra/3269.

26. N. A. Manikandan, K. Pakshirajan, and G. Pugazhenthi, "Techno-economic Assessment of a Sustainable and Cost-effective Bioprocess for Large Scale Production of Polyhydroxybutyrate," *Chemosphere* 284 (2021): 131371, https://doi.org/10.1016/j.chemosphere.2021.131371.

27. M. T. Aminzai, N. Azizi, Y. Nural, and E. Yabalak, "A Review on Recent Advances in Polymer-Assisted Green and Sustainable Technology for Remediation of Pharmaceuticals from Water and Wastewater," *Water, Air, & Soil Pollution* 234 (2023): 681, https://doi.org/10.1007/s11270-023-06698-7.

28. R. Singh and A. Sinha, "A Critical Review of Recent Advancements in the Photocatalysis Process, Mechanism, and Degradation Pathways for the Removal of Phthalates from the Contaminated Water Matrix," *Journal of Environmental Management* 377 (2025): 124663, https://doi.org/10.1016/j.jenvman.2025.124663.

29. M. Cantarella, G. Impellizzeri, A. Di Mauro, V. Privitera, and S. C. Carroccio, "Innovative Polymeric Hybrid Nanocomposites for Application in Photocatalysis," *Polymers* 13 (2021): 1184, https://doi.org/10.3390/polym13081184.

30. C. Zarzzeka, J. Goldoni, J. D. R. D. Oliveira, G. G. Lenzi, M. D. Bagatini, and L. M. S. Colpini, "Photocatalytic Action of Ag/TiO_2 Nanoparticles to Emerging Pollutants Degradation: A Comprehensive Review," *Sustainable Chemistry for the Environment* 8 (2024): 100177, https://doi.org/10.1016/j.scenv.2024.100177.

31. R. Bianchini, G. Cevasco, C. Chiappe, C. S. Pomelli, and M. J. Rodrıǵuez Douton, "Ionic Liquids Can Significantly Improve Textile Dyeing: An Innovative Application Assuring Economic and Environmental Benefits," *ACS Sustainable Chemistry & Engineering* 3 (2015): 2303–2308.

32. S. Marullo and F. D'Anna, "Combining Carbon Materials and Ionic Liquid Gels to Boost Simultaneous Removal of Emerging Pollutants from Wastewaters," *Advanced Sustainable System* 8 (2024): 2300639, https://doi.org/10.1002/adsu.202300639.

33. C. Rizzo, S. Marullo, P. R. Campodonico, et al., "Self-Sustaining Supramolecular Ionic Liquid Gels for Dye Adsorption," *ACS Sustainable Chemistry & Engineering* 6 (2018): 12453–12462, https://doi.org/10.1021/acssuschemeng.8b03002.

34. S. Marullo, C. Rizzo, N. T. Dintcheva, F. Giannici, and F. D'Anna, "Ionic Liquids Gels: Soft Materials for Environmental Remediation,"

Journal of Colloid and Interface Science 517 (2018): 182–193, https://doi.org/10.1016/j.jcis.2018.01.111.

35. K. Y. Law, "Definitions for Hydrophilicity, Hydrophobicity, and Superhydrophobicity: Getting the Basics Right," *The Journal of Physical Chemistry Letters* 5 (2014): 686–688, https://doi.org/10.1021/jz402762h.

36. J. Wang and X. Guo, "Adsorption Kinetic Models: Physical Meanings, Applications, and Solving Methods," *Journal of Hazardous Materials* 390 (2020): 122156, https://doi.org/10.1016/j.jhazmat.2020.122156.

37. E. D. Revellame, D. L. Fortela, W. Sharp, R. Hernandez, and M. E. Zappi, "Adsorption Kinetic Modeling Using Pseudo-first Order and Pseudo-second Order Rate Laws: A Review," *Cleaner Engineering and Technology* 1 (2020): 100032–100032, https://doi.org/10.1016/j.clet.2020.100032.

38. D. Posada and T. R. Buckley, "Model Selection and Model Averaging in Phylogenetics: Advantages of Akaike Information Criterion and Bayesian Approaches over Likelihood Ratio Tests," *Systematic Biology* 53 (2004): 793–808, https://doi.org/10.1080/10635150490522304.

39. J. T. de Oliveira, K. G. P. Nunes, D. Cardoso Estumano, and L. A. Féris, "Applying the Bayesian Technique, Statistical Analysis, and the Maximum Adsorption Capacity in a Deterministic Way for Caffeine Removal by Adsorption: Kinetic and Isotherm Modeling," *Industrial & Engineering Chemistry Research* 63 (2024): 1530–1545.

40. J. P. Vareda, "On Validity, Physical Meaning, Mechanism Insights and Regression of Adsorption Kinetic Models," *Journal of Molecular Liquids* 376 (2023): 121416–121416, https://doi.org/10.1016/j.molliq.2023.121416.

41. M. Alkhabbas, A. M. Al-Ma'abreh, G. Edris, T. Saleh, and H. Alhmood, "Adsorption of Anionic and Cationic Dyes on Activated Carbon Prepared from Oak Cupules: Kinetics and Thermodynamics Studies," *International Journal of Environmental Research and Public Health* 20 (2023): 3280–3280, https://doi.org/10.3390/ijerph20043280.

42. X. Jin, J. Talbot, and N.-H. L. Wang, "Analysis of Steric Hindrance Effects on Adsorption Kinetics and Equilibria," *AIChE Journal* 40 (1994): 1685–1696, https://doi.org/10.1002/aic.690401010.

43. J. Wang and X. Guo, "Adsorption Isotherm Models: Classification, Physical Meaning, Application and Solving Method," *Chemosphere* 258 (2020): 127279, https://doi.org/10.1016/j.chemosphere.2020.127279.

44. S. Cataldo, A. Gianguzza, A. Pettignano, and I. Villaescusa, "Mercury(II) Removal from Aqueous Solution by Sorption onto Alginate, Pectate and Polygalacturonate Calcium Gel Beads. A Kinetic and Speciation Based Equilibrium Study," *Reactive and Functional Polymers* 73 (2013): 207–217, https://doi.org/10.1016/j.reactfunctpolym.2012.10.005.

45. S. Cataldo, N. Muratore, F. Giannici, et al., "Hydrocarbons Removal from Synthetic Bilge Water by Adsorption onto Biochars of Dead Posidonia oceanica," *Environmental Science and Pollution Research* 29 (2022): 90231–90247, https://doi.org/10.1007/s11356-022-21998-x.

46. D. Liu, J. Yuan, J. Li, and G. Zhang, "Preparation of Chitosan Poly(methacrylate) Composites for Adsorption of Bromocresol Green," *ACS Omega* 4 (2019): 12680–12686, https://doi.org/10.1021/acsomega.9b01576.

47. J. Saleem, Z. K. B. Moghal, S. Pradhan, et al., "Adsorbent-Embedded Polymeric Membranes for Efficient Dye-Water Treatment," *Polymers* 16 (2024): 1459, https://doi.org/10.3390/polym16111459.

48. A. K. El-Sawaf, A. A. Nassar, A. A. El Aziz Elfiky, and M. F. Mubarak, "Advanced Microcrystalline Nanocellulose-Based Nanofiltration Membranes for the Efficient Treatment of Wastewater Contaminated with Cationic Dyes," *Polymer Bulletin* 81 (2024): 12451–12476, https://doi.org/10.1007/s00289-024-05279-w.

49. W. Xiang, Q. Wang, Z. Li, et al., "Water-Stable Methyl-Modified MOF and Mixed Matrix Membrane for Efficient Adsorption and Separation of Cationic Dyes," *Separation and Purification Technology* 330 (2024): 125268, https://doi.org/10.1016/j.seppur.2023.125268.

50. A. V. B. Reddy, R. Rafiq, A. Ahmad, A. S. Maulud, and M. Moniruzzaman, "Cross-Linked Ionic Liquid Polymer for the Effective Removal of Ionic Dyes from Aqueous Systems: Investigation of Kinetics and Adsorption Isotherms," *Molecules* 27 (2022): 7775, https://doi.org/10.3390/molecules27227775.

51. A. P. Heitmann, I. C. Rocha, P. P. de Souza, L. C. A. Oliveira, P. S. de, and O. Patrício, "Photoactivation of a Biodegradable Polymer (PHB): Generation of Radicals for Pollutants Oxidation," *Catalysis Today* 344 (2020): 171–175, https://doi.org/10.1016/j.cattod.2018.12.024.

52. M. N. Chong, B. Jin, C. W. K. Chow, and C. Saint, "Recent Developments in Photocatalytic Water Treatment Technology: A Review," *Water Research* 44 (2010): 2997–3027, https://doi.org/10.1016/j.watres.2010.02.039.

53. F. D'Anna, S. Marullo, P. Vitale, and R. Noto, "The Effect of the Cation π-Surface Area on the 3D Organization and Catalytic Ability of Imidazolium-Based Ionic Liquids," *European Journal of Organic Chemistry* 2011 (2011): 5681–5689.

Supporting Information

Additional supporting information can be found online in the Supporting Information section.

Supporting File: adsu70596-sup-0001-SuppMat.pdf.